

# Marginal Methods of IDF Estimation in Scaling and Non-Scaling Rainfall

By

Daniele Veneziano<sup>1</sup>, Chiara Lepore<sup>2</sup>, Andreas Langousis<sup>1</sup>, and Pierluigi Furcolo<sup>2</sup>

<sup>1</sup>Department of Civil and Environmental Engineering  
Massachusetts Institute of Technology  
Cambridge, Massachusetts, 02139, U.S.A.

<sup>2</sup>Dipartimento di Ingegneria Civile  
Università degli Studi di Salerno  
Fisciano (SA) 84084, Italy

Submitted to

*Water Resources Research*

Originally Submitted March, 2007

Revised June, 2007

-----  
Correspondence: Andreas Langousis, Dept. of Civil and Environmental Engineering, MIT, Room 1-245,  
Cambridge, MA 02139. Phone : (617)407-0059, Fax: (440)756-2310, e-mail: andlag@mit.edu.

## Abstract

Practical methods for the estimation of the Intensity-Duration-Frequency (IDF) curves are usually based on the observed annual maxima of the rainfall intensity  $I(d)$  in intervals of different duration  $d$ . Using these historical annual maxima, one estimates the IDF curves under the condition that the rainfall intensity in an interval of duration  $d$  with return period  $T$  is the product of a function  $a(T)$  of  $T$  and a function  $b(d)$  of  $d$  (separability condition). Various parametric or semi-parametric assumptions on  $a(T)$  and  $b(d)$  produce different specific methods. As alternatives, we develop IDF estimation procedures based on the marginal distribution of  $I(d)$ . If the marginal distribution scales in a multifractal way with  $d$ , this condition can be incorporated. We also consider hybrid methods that estimate the IDF curves using both marginal and annual-maximum rainfall information. We find that the separability condition does not hold and that the marginal and hybrid methods perform better than the annual-maximum estimators in terms of accuracy and robustness relative to outlier rainfall events. This is especially true for long return periods and when the length of the available record is short. Marginal and hybrid methods produce accurate IDF estimates also when only a few years of continuous rainfall data are available.

**Keywords:** rainfall extremes, IDF curves, rainfall scaling, multifractal processes

## 1. Introduction

The estimation of rainfall extremes, as embodied in the Intensity-Duration-Frequency (IDF) curves, has been a central problem of hydrology since the early work of Sherman (1931) and Bernard (1932); see for example Eagleson (1970), Chow *et al.* (1988) and Singh (1992). The IDF curves are defined as follows. Let  $I(d)$  be the average rainfall intensity in a generic interval of duration  $d$ ,  $I_{\max}(d)$  be the annual maximum of  $I(d)$ , and  $i_{\max}(d, T)$  be the value exceeded by  $I_{\max}(d)$  on average every  $T$  years. The IDF curves are plots of  $i_{\max}$  against  $d$  for different values of  $T$ .

Standard IDF estimation methods make assumptions directly on the function  $i_{\max}(d, T)$  and fit its parameters to the historical annual maxima; see Koutsoyiannis *et al.* (1998) for a review and Section 2 below for two specific methods. In most cases  $i_{\max}(d, T)$  is taken to be a separable function of  $d$  and  $T$ ,

$$i_{\max}(d, T) = a(T) \cdot b(d) \quad (1)$$

where the functions  $a(T)$  and  $b(d)$  are assumed to have some parametric form. The methods are simple and widely used, since they implicitly account for the yearly rainfall cycle, do not require continuous records, and allow one to consider the data as a sample of independent realizations of the same random variable, thus providing a rationale for choosing a probabilistic model based on extreme value theory (Gumbel, 1958; Coles, 2001).

The drawbacks of the annual-maximum methods are also well known (Coles and Tawn, 1996; Coles *et al.*, 2003): these methods make poor use of the data when continuous records are available, lack robustness when extrapolating to high return periods, and fit extreme value distributions to data that are still far from the asymptotic

regime. Another limitation comes from using Eq. 1, as there is evidence that this separability condition does not hold (see Section 4.1).

Many meteorological stations have replaced the old mechanical rain gauges with electronic gauges, which greatly facilitate the recording and storing of continuous rainfall data. This innovation poses the interesting new problem of how to use continuous data to refine the estimation of the IDF curves. A technique that addresses this problem is the “peaks over threshold” (POT) method (Davison and Smith, 1990; Rosbjerg and Madsen, 1995; Madsen *et al.*, 1997a; b). By using the values that exceed a sufficiently high threshold, the POT technique includes rainfall values that, although not themselves annual maxima, belong to the right tail of the distribution of rainfall intensity. The larger samples produce estimators of the IDF curves that are more accurate and robust than those from annual-maximum data alone; see Katz *et al.* (2002) and Madsen *et al.*, (1997a, b) for a comparison.

Issues with the POT method are the selection of the threshold (Rosbjerg and Madsen, 1992; Lang *et al.*, 1999) and the fact that again only a fraction of the information in continuous rainfall records is used. Therefore, in spite of the increased accuracy of the POT procedure, the problem of fitting annual maximum distributions to continuous rainfall data cannot be considered completely solved. One possibility is to fit a stochastic rainfall model to the continuous rainfall record and estimate the IDF curves from the fitted model; see for example Chow *et al.* (1988), Singh (1992), Cowpertwait (1995, 1998), and Willems (2000). However, this approach is more complex than direct IDF estimation from annual maxima and POT values: the number of parameters is larger, their estimation is often more laborious, and finding the IDF curves typically requires

extensive model simulation. A notable exception is when the rainfall model has multifractal scale invariance (Schertzer and Lovejoy, 1987; Lovejoy and Schertzer, 1995; Olsson, 1995; Veneziano and Iacobellis, 2002). The reason is that scale invariance reduces the number of parameters, simplifies model fitting, and makes it possible to obtain the distribution of  $I_{\max}(d)$  by semi-analytical methods (Veneziano *et al.*, 2006; Langousis and Veneziano, 2007). Even simpler IDF estimation procedures based on scaling of the marginal moments of  $I(d)$  are introduced in Section 3.2. One objective of this study is to compare these simple multifractal methods to standard annual-maximum procedures for practicality, accuracy, robustness and data need.

The physical origin of scale invariance in rainfall is not well understood, although linkage is often made to the multifractality of atmospheric turbulence (Lovejoy and Schertzer, 1990; 1995). Multifractal scale invariance has been observed in both convective and stratiform rainfall, with small differences in the scaling parameters (Willems, 2000). In temperate climates, the scaling range may extend from about 1 hour to a few days (Burlando and Rosso, 1996; Willems, 2000; Veneziano and Iacobellis, 2002; Koutsoyiannis, 2006), whereas in tropical climates and in general when diurnal convection dominates, the upper limit of the scaling range may reduce to just a few hours (the characteristic duration of such diurnal convective events); see for example the Yangambi, Binja and Ndjili records in Mohyont *et al.* (2004). Outside the scaling range, the fluctuations of rainfall intensity are generally smaller than under multifractality (Fraedrich and Larnder, 1993; Olsson, 1995; Onof *et al.*, 1996; Menabde *et al.*, 1997; de Lima and Grasman, 1999; Menabde and Sivapalan, 2000). This motivates our second

objective, which is to extend the multifractal IDF methods to durations  $d$  for which rain is non-scaling. Also this extension is based on the marginal moments of  $I(d)$ .

Finally, we consider hybrid methods in which the distribution of  $I_{\max}(d)$  from marginal (scaling or non-scaling) analysis is corrected such that its mean value matches the average of the historical annual maxima. This is a practical way to utilize the information on both the marginal and extremal properties of rainfall while correcting the marginal methods for the effects of dependence of rainfall in different  $d$  intervals and the overlap of the  $d$  intervals themselves.

Numerical evaluations are made using historical records from Heathrow Airport (UK), Walnut Gulch (Arizona) and Florence (Italy), and one synthetic 1000-yr record generated by a rainfall simulator with known IDF curves. Basic characteristics of these records are as follows.

The Heathrow record is an hourly time series covering the period from 1949 to 2001. Two years, 1988 and 2001, are incomplete and are excluded from the analysis, which is therefore based on 51 years. The reduced time series includes two years, 1959 and 1970, when the maximum rainfall intensity for short durations was especially intense, not just at the Heathrow Airport but over most of Southern England; see [http://www.personal.dundee.ac.uk/~taharley/1959\\_weather.htm](http://www.personal.dundee.ac.uk/~taharley/1959_weather.htm) and [/1970\\_weather.htm](http://www.personal.dundee.ac.uk/~taharley/1970_weather.htm)). When assessing the sensitivity of different methods to “outlier years”, we have compared results with and without 1959 and 1970.

The Walnut Gulch time series refers to gage No. 42 of Watershed 63 (Walnut Gulch) and is available at <http://www.tucson.ars.ag.gov/dap/DataCatalogueOld.htm>. This site reports total rain depths during rainy periods of variable durations. For our analysis we

first disaggregated the historical record into 1-min values (assuming constant rainfall intensity in each reported rainy period) and then aggregated the record at the hourly scale. The total length of the record is 49 years, with no particular year recognized as an outlier.

The Florence record comprises 24 years, from 1962 to 1985, and has a 5-min nominal resolution (Becchi and Castelli, 1989). However, the values at this fine resolution have limited accuracy and for the present analysis the data have been aggregated at the hourly scale. One year, 1966, includes an event that caused a catastrophic flood in Florence. The flood is the most severe since 1173, the starting year of the Arno River flood record (Caporali *et al.*, 2005). Our analysis (see Section 4.2) shows that for long durations the rainfall intensity during that event has a return period of about 500 years. Hence, when we analyze sensitivity to outlier years, we remove year 1966. Also other years display somewhat unusual rainfall patterns, with high maximum rainfall intensities at either short durations (1985) or very long durations (1973). Since these intensities have an estimated return period of about 100 years, they cannot be characterized as outliers in a 24-year record and are never excluded.

The 1000-year synthetic record was obtained using a multifractal model of the beta-lognormal type (“Model 3” of Langousis and Veneziano, 2007). The model is simply a sequence of independent multiplicative cascades with three parameters: the maximum temporal scale  $d_{\max}$  for which multifractality applies ( $d_{\max}$  is on the order of 7-15 days), and two parameters,  $C_\beta$  and  $C_{LN}$ , that describe the scaling of rainfall inside each  $d_{\max}$  interval. Specifically,  $C_\beta$  controls the fractal dimension ( $1-C_\beta$ ) of the rain support, whereas  $C_{LN}$  controls the amplitude of the intensity fluctuations when it rains. For additional details, see Langousis and Veneziano (2007). Using this model, each synthetic

year was constructed as a sequence of 38 independent and statistically identical cascade realizations with  $d_{\max} = 9.56$  days. Each cascade was developed to a maximum resolution of 3.36 min and then aggregated at the hourly level. The scaling parameters,  $C_{\beta} = 0.46$  and  $C_{LN} = 0.06$ , were chosen by fitting the model to the 24-year Florence record.

Basic statistics of the actual and synthetic records are given in Tables 1 and 2. The rainfall climate of Walnut Gulch is much drier than those of Florence and Heathrow; see the mean rainfall intensity and the rainy fraction. However, the mean rainfall intensity during the rainy periods is maximum at Walnut Gulch, followed by Florence and finally Heathrow. This reflects the relative importance of convective rainfall at the three sites. These climatic features are reflected in the 1-hr and 24-hr statistics reported in Tables 2a and 2b, in particular the mean of the annual maxima. The skewness coefficient for Walnut Gulch is much lower than that for Florence and Heathrow, because for durations of 1 and 24 hours the historical annual maxima for Walnut Gulch display a short upper tail. Notice also the high sensitivity of the 24-hour annual maximum statistics for Florence to the inclusion/exclusion of the year 1966 and the somewhat lower sensitivity of the 1-hr annual maximum statistics for Heathrow to the inclusion/exclusion of years 1959 and 1970.

The paper is organized as follows. Section 2 describes the annual-maximum approaches to IDF curve estimation considered in this study and Section 3 describes marginal multifractal, marginal non-scaling and hybrid alternatives. Section 4 makes a detailed comparison of the methods using the rainfall records mentioned above. Conclusions and practical recommendations are given in Section 5.



## 2. IDF Estimation Methods Based on Annual Maxima

Direct approaches to IDF-curve estimation differ mainly in their parameterization of the functions  $a(T)$  and  $b(d)$  in Eq. 1. Some methods parameterize both functions, while others express dependence on  $T$  in a nonparametric or semi-parametric way. A representative method of each type is described below. For further details and variants of these procedures, see Demarée (1985) and Koutsoyiannis *et al.* (1998).

### 2.1 Semi-Parametric Annual-Maximum Method

Semi-parametric annual-maximum (SPM) procedures start by assuming a distribution type for the annual maximum intensity  $I_{\max}(d)$ , which is equivalent to specifying a parametric form for  $a(T)$  in Eq. 1. The most popular assumption is that  $I_{\max}(d)$  has extreme-value distribution of the first or second type (EV1 or EV2), although other distributions have also been used (Koutsoyiannis *et al.*, 1998). The EV1 and EV2 models are special cases of the Generalized Extreme Value (GEV) distribution

$$F(x) = \exp\left\{-\left[1 + k\left(\frac{x - \psi}{\lambda}\right)\right]^{-1/k}\right\} \quad (2)$$

where  $k$ ,  $\psi$  and  $\lambda$  are shape, location and scale parameters, respectively. For  $k = 0$ , Eq. 2 reduces to the Gumbel (EV1) distribution  $F(x) = \exp\{-\exp(-(x - \psi)/\lambda)\}$ , whereas for positive and negative  $k$  the distribution is respectively Frechet (EV2) and Weibull (EV3). Since it is difficult to determine from theory to which extreme type the rainfall maxima are attracted, several recent studies have hypothesized that  $I_{\max}(d)$  has GEV distribution and let all three parameters (including  $k$ ) vary with  $d$  (Parrett, 1997; Asquith, 1998; Baillon *et al.*, 2004; Mohymont *et al.*, 2004; Trefry *et al.*, 2005; Vaskova and Francis 2000; Bessemoulin P., 2006, personal communication). This is also what we do here.

Common estimation procedures for  $\{k, \psi, \lambda\}$  are the method of moments, the method of probability-weighted moments (PWM), and maximum likelihood. Here we use the PWM method, due to its higher robustness against outliers (Hosking, 1992; Vogel and Fennessey, 1993; Sankarasubramanian and Srinivasan, 1999). Using the parameters  $\{k, \psi, \lambda\}$  estimated for each duration  $d$ , a first estimate of the IDF curves  $i_{\max}(d, T)$  is obtained as the  $(1-1/T)$ -quantile of  $F$  in Eq. 2. This gives

$$i_{\max}(d, T) = \begin{cases} \psi + \frac{\lambda}{k} \left\{ \left[ -\ln\left(1 - \frac{1}{T}\right) \right]^{-k} - 1 \right\}, & \text{for } k \neq 0 \\ \psi - \lambda \ln \left[ -\ln\left(1 - \frac{1}{T}\right) \right], & \text{for } k = 0 \end{cases} \quad (3)$$

The estimates in Eq. 3 depend in a non-smooth way on  $d$  and are highly variable, especially for long return periods  $T$ . In the final step, statistical variability is reduced by fitting a model of the type in Eq. 1 with parametric  $b(d)$  and nonparametric  $a(T)$  to the  $i_{\max}(d, T)$  estimates. A popular choice for  $b(d)$  is the power function

$$b(d) = \frac{1}{(d + \delta)^\eta} \quad (4)$$

where  $\delta$  and  $\eta$  are non-negative parameters (Koutsoyiannis *et al.*, 1998). Estimation of  $\delta$ ,  $\eta$  and  $a(T)$  (one  $a$  parameter for each  $T$ ) is by least-squares fitting of the  $\log[i_{\max}(d, T)]$  values in Eq. 3. The final IDF model is separable, parametric in  $d$  and nonparametric in  $T$ , although dependence on  $T$  reflects in part the initial assumption that  $I_{\max}(d)$  has a GEV distribution.

## 2.2 Parametric Annual-Maximum Method

Completely parametric annual-maximum (CPM) alternatives assume that both  $a(T)$  and  $b(d)$  in Eq. 1 are known except for a few parameters. Equation 4 is again the most frequent specification for  $b(d)$ . The function  $a(T)$  is sometimes taken to have power or logarithmic form (Chow *et al.*, 1988; Singh, 1992), but as Rossi and Villani (1994) and Koutsoyiannis *et al.* (1998) have argued, a better approach is to derive  $a(T)$  from an assumed distribution of the reduced annual maximum intensity  $Y = I_{\max}(d)/b(d)$ . Under Eq. 1, the distribution of  $Y$  does not depend on  $d$  and all observed values of  $Y$  can be pooled to estimate this distribution. As for  $I_{\max}(d)$  in the semi-parametric method, we assume that  $Y$  has a GEV distribution of the type in Eq. 2. Once this distribution  $F$  has been estimated, the function  $a(T)$  is obtained as  $a(T) = F^{-1}(1 - 1/T)$ , which is the expression on the right hand side of Eq. 3.

Koutsoyiannis *et al.* (1998) describe two robust techniques for estimating the parameters of  $b(d)$  and  $a(T)$ , which are referred to as the one-step and two-step procedures. We have found that results from the two methods are very similar and decided to retain the two-step approach for numerical analysis. This approach estimates first the parameters of  $b(d)$  and then the parameters of  $a(T)$ . The first step is accomplished by minimizing the Kruskal-Wallis index for the samples of reduced annual maxima  $Y(d)$  and the second step fits a GEV distribution to the combined set of  $Y(d)$  values; for details see Koutsoyiannis *et al.* (1998).

## 3. Marginal and Hybrid IDF Estimation Methods

The main focus of this study is the use of marginal-distribution and hybrid alternatives to the annual-maximum methods described above. Marginal-distribution methods consist of

estimating the marginal distribution  $F_{I(d)}$  of the average rainfall intensity in  $d$  and then finding the distribution of the annual maximum  $I_{\max}(d)$  as

$$F_{I_{\max}(d)}(i) = [F_{I(d)}(i)]^{1/d} \quad (5)$$

where  $d$  is in years. The IDF value  $i_{\max}(d, T)$  is found as the  $(1-1/T)$ -quantile of  $I_{\max}(d)$ .

Equation 5 makes the simplifying assumption that the maximum annual rainfall occurs in one of the  $1/d$  non-overlapping intervals into which the year is partitioned and further assumes independence of rainfall in different intervals. Ways to correct for the bias from these simplifying assumptions are described in Section 3.3, where we also introduce hybrid methods.

### ***3.1 Marginal Method for Non-Scaling Rainfall***

What matters for the calculation of  $F_{I_{\max}(d)}$  through Eq. 5 is the accurate estimation of  $F_{I(d)}$  in the upper tail. As we show next, this upper tail is well approximated by a lognormal shape, as in distributions of the type

$$F_{I(d)}(i) = P_0 + (1 - P_0)\Phi\left(\frac{\ln i - m}{\sigma}\right) \quad (6)$$

where  $\Phi$  is the standard normal CDF and  $(0 < P_0 < 1, m, \sigma > 0)$  are parameters that depend on  $d$ . According to Eq. 6, there is a probability  $P_0$  that a generic  $d$  interval is dry and the rainfall intensity in the wet intervals has lognormal distribution. At low intensities, the empirical distribution of  $[I(d) | I(d) > 0]$  usually differs from a lognormal distribution, but we emphasize that here Eq. 6 is used for its upper tail; hence  $P_0$  is just a parameter that controls the thickness of the upper tail and needs not agree with the empirical relative frequency of dry conditions. The moments of  $I(d)$  in Eq. 6 are

$$\mu_{q,d} = E[I(d)^q] = (1 - P_0) \exp\left\{qm + \frac{1}{2}q^2\sigma^2\right\} \quad (7)$$

For each given  $d$ , the parameters  $(P_0, m, \sigma^2)$  can be found by matching three empirical moments of  $I(d)$ , chosen among those sensitive to the upper tail of the empirical distribution. Using the moments of order  $q = 1, 2$  and  $3$ , Eq. 7 gives

$$\begin{aligned} P_0 &= 1 - \mu_{3,d} \left(\frac{\mu_{1,d}}{\mu_{2,d}}\right)^3 \\ m &= \ln\left[\frac{\mu_{2,d}^4}{\mu_{3,d}^{3/2} \mu_{1,d}^{5/2}}\right] \\ \sigma^2 &= \ln\left[\frac{\mu_{3,d} \mu_{1,d}}{\mu_{2,d}^2}\right] \end{aligned} \quad (8)$$

The use of moments of order  $q \geq 4$  is not recommended due to their higher sampling variability.

Figure 1 uses the historical and synthetic records to show how Eq. 6 with parameters in Eq. 8 fits the upper tail of the empirical distribution of  $I(d)$ . For each record and each of two durations ( $d = 1$  hr and  $d = 24$  hr), the theoretical exceedance probability from Eq. 6 is plotted against the empirical exceedance probability. For convenience, both probabilities are divided by  $(1 - P_{0,emp})$ , the empirical fraction of wet  $d$  intervals. The plots are constructed as follows. For each observed value of  $I(d)$  one finds the empirical exceedance probability  $P_{emp}$  using Weibull's plotting position and the theoretical exceedance probability  $P_{th}$  using Eqs. 6 and 8. Figure 1 plots  $P_{th}/(1 - P_{0,emp})$  against  $P_{emp}/(1 - P_{0,emp})$  for  $P_{emp}/(1 - P_{0,emp}) \leq 0.25$ . The fact that the plots deviate little from the dashed 45-degree lines supports the assumption of a lognormal upper tail. This is a significant finding, since the good fit is observed for different durations and different

rainfall climates. Figure 1 also shows that fitting Eq. 6 using the first three moments reproduces well the empirical distribution of  $I(d)$  in the range of the empirical annual maxima; see double-headed arrows.

When they are obtained directly from the sample, the moments  $\mu_{q,d}$  in Eq. 8 need not scale with or depend in any particular way on duration  $d$ . Therefore this marginal procedure can be used without any assumption of scaling of the rainfall process. We call this the local marginal (LM) method. While all the marginal-distribution analyses presented in this paper are based on the assumption of a lognormal upper tail, the approach can be readily adapted for cases when other distribution types are more appropriate.

### ***3.2 Multifractal Methods for Scaling Rainfall***

In the case when rainfall has multifractal scale invariance, the moments  $E[I(d)^q]$  vary with  $d$  as

$$E[I(d)^q] = E[I(d_{\max})^q] \cdot \left(\frac{d}{d_{\max}}\right)^{-K(q)}, \quad d \leq d_{\max} \quad (9)$$

where  $K(q)$  is a moment scaling function and  $d_{\max}$  is the upper limit of the scaling range. For multifractal models of temporal rainfall, see for example Schertzer and Lovejoy (1987), Lovejoy and Schertzer (1995), Olsson (1995), Menabde *et al.* (1997), Schmitt *et al.* (1998), de Lima and Grasman (1999), Menabde and Sivapalan (2000), Willems (2000), Veneziano and Iacobellis (2002), and Langousis and Veneziano (2007).. Technically, the scaling range cannot have a positive lower limit, but in practice one observes that Eq. 9 holds in good approximation for  $d$  above some positive value  $d_{\min}$ .

The scaling range  $[d_{\min}, d_{\max}]$  is found from log-log plots of the empirical moments of  $I(d)$  against  $d$ .

The moment-scaling property in Eq. 9 can be used in various ways to reduce the number of parameters and add robustness to the IDF estimation procedure described in Section 3.1. The simplest way is to obtain the moments needed in Eq. 8 by fitting straight log-log lines to the empirical moments of order 2 and 3 inside the scaling range. This operation produces smoother IDF curves than using the empirical moments for each duration  $d$ . We call this the multifractal marginal (MFM) method.

Figure 2 shows log-log plots of the normalized empirical moments  $E\{[I(d)/\bar{I}]^q\}$  against  $d$  for  $q = 0, 1, 2, 3$  and 4 for the four records. Normalization is by the empirical average rain rate  $\bar{I}$ , the values of which are given in the figure. For each data set, the range over which the moments of order 2 and 3 scale is identified and power law functions are fitted using linear regression (solid lines).

The fitted normalized moments and the average intensities  $\bar{I}$  are used by the MFM method. The dashed lines in Figure 2 are obtained by inserting the fitted moments into Eq. 8 to obtain the parameters  $(P_0, m, \sigma^2)$  and then using Eq. 7 to calculate the moments of order 0 and 4. As one can see, the moments of order 4 of the historical records are slightly overpredicted (this is because the 4<sup>th</sup> order moments from relatively small samples tend to be lower than the corresponding theoretical moments). Also notice that for the same records the probability at 0 is overestimated, because the body and lower tail of the empirical distribution are thicker than those of the lognormal distribution fitted through Eq. 8. All moments of the synthetic record are accurately reproduced.

The MFM procedure presented here is a simplified version of the multifractal IDF estimation methods proposed by Langousis and Veneziano (2007) and Langousis *et al.* (2007). The main difference is that here we ignore the fact that the so-called dressing factor prevents a multifractal process from having marginal distributions of the type in Eq. 6 with exponential upper tails. Rather, under multifractality, the marginal distribution of  $I(d)$  has a power-law upper tail. However, this power-law tail applies only to extreme quantiles, which are beyond the range that is typically of interest for IDF estimation (Langousis *et al.*, 2007) and in practice Eq. 6 holds in very good approximation; see the excellent lognormal fits to the tails of  $I(d)$  for the synthetic record in Figure 1.

### ***3.3 Bias Corrections and Hybrid Methods***

As was mentioned at the beginning of Section 3, IDF estimates based on Eq. 5 are biased by the assumptions that: 1. the maximum annual rainfall occurs in one of the non-overlapping  $d$  intervals and 2. rainfall amounts in different  $d$  intervals are independent. The classical way to eliminate the first source of bias is to multiply  $I_{\max}(d)$  in Eq. 5 by a continuity correction factor  $R_{cont}(d)$ . Several studies (Hershfield, 1961, Weiss, 1964; Young and McEnroe, 2003) have shown that  $R_{cont}(d)$  is about 1.13-1.15. Similarly, one may apply a correction factor  $R_{dep}(d)$  for dependence.

Figure 3 shows how, for each duration  $d$ , one can use a rainfall record to estimate  $R_{cont}$  and  $R_{dep}$  and the combined correction factor  $R = R_{cont} \cdot R_{dep}$ . For method MFM, these factors are estimated as



$$\begin{aligned}
R_{cont} &= \frac{\bar{I}_{\max,overlap}}{\bar{I}_{\max,no-overlap}} \\
R_{dep} &= \frac{\bar{I}_{\max,no-overlap}}{m_{I_{\max,MFM}}} \\
R &= R_{cont} \cdot R_{dep} = \frac{\bar{I}_{\max,overlap}}{m_{I_{\max,MFM}}}
\end{aligned} \tag{10}$$

where  $\bar{I}_{\max,overlap}$  and  $\bar{I}_{\max,no-overlap}$  are the empirical average annual maxima with and without  $d$ -interval overlapping, respectively, and  $m_{I_{\max,MFM}}$  is the mean value of  $I_{\max}(d)$  in Eq. 5 when  $F_{I(d)}$  is estimated by the MFM method. A similar procedure applies to the LM method.

The factor  $R_{cont}$  in Figure 3 fluctuates around 1.13, as expected, whereas  $R_{dep}$  is close to 1, indicating no significant bias from assuming independence. The latter result confirms the findings of Veneziano and Langousis (2005) for multifractal rainfall. When rainfall is multifractal, one can calculate the exact distribution of the annual maximum  $I_{\max}(d)$  using a numerical procedure that accounts for dependence. Veneziano and Langousis (2005) compared the exact results with the approximation in Eq. 5 and concluded that the effect of dependence on the IDF curves is small, especially for long return periods  $T$ . Hence it is accurate to correct for all biases of the marginal LM and MFM methods by multiplying the IDF estimates from Eq. 5 by 1.13.

When the correction factor  $R(d)$  is not fixed but is estimated using Eq. 10 with  $\bar{I}_{\max,overlap}(d)$  from at-site annual maximum data, we refer to the corrected IDF estimates as hybrid LM/H or MFM/H estimates. The term hybrid indicates that the estimates are based on both marginal and annual-maximum information. Use of only the average value of the annual maxima is justified by the fact that, especially for short rainfall records, the

shape of the annual maximum distribution is better estimated from marginal information than from extreme value information, whereas the mean value can be reliably found from the annual maxima. One would expect the hybrid method to be superior to just fixing  $R(d)$  to 1.13 when long annual-maximum records are available, whereas the reverse should be true for short annual-maximum records. For a quantitative analysis, see Section 4.3.

#### **4. Comparison of Annual-Maximum, Marginal and Hybrid IDF Estimates**

In this section we apply the two annual-maximum methods (semi-parametric SPM and completely parametric CPM), two marginal-moment methods (local LM and multifractal MFM, both with continuity correction factor 1.13), and the hybrid method MFM/H to the actual and synthetic records. We are especially interested in assessing the separability condition in Eq. 1, the sensitivity of each method to “outlier years”, and the stability of the results when only a few years of data are available.

##### ***4.1 The Assumption of Separability***

The annual-maximum methods described in Section 2 assume that the IDF values are separable, in the sense that they are affected in an independent multiplicative way by the duration  $d$  and the return period  $T$ ; see Eq. 1. On the other hand, multifractal analysis suggests that this is true only under the asymptotic conditions  $d \rightarrow 0$  or  $T \rightarrow \infty$ , whereas for nonzero  $d$  and finite  $T$  the IDF values are more sensitive to  $T$  when  $d$  is small than when  $d$  is large (Veneziano and Furcolo, 2002; Langousis and Veneziano, 2007; Langousis *et al.*, 2007).

There is convincing evidence that the separable IDF structure in Eq. 1 does not hold and the multifractal predictions are qualitatively correct. For example, one may consider

the shape parameter  $k$  of the GEV distribution in Eq. 2. Under the separability condition  $k$  is constant with  $d$ , whereas under the non-separability predicted by multifractal analysis  $k$  decreases as  $d$  increases. Figure 4 shows  $k(d)$  functions for the actual and synthetic records used here (dotted lines) and a few  $k(d)$  functions from the literature, chosen to be those based on larger data sets (solid lines). For Florence, the values of  $k$  for  $d \geq 1$  hr use 47 years of annual maximum data (Caporali *et al.*, 2006), whereas for  $d < 1$  hr the data cover the 24-year period (1962-1985) used in the present study. For all the present records and most of the records in the literature, the  $k$  parameter was estimated using probability-weighted moments (Hosking, 1992).

In general,  $k$  peaks for  $d$  around 1-3 hr and decays for shorter and longer durations. The decay for longer durations agrees well with the trend produced by multifractal rainfall models (see results in Figure 4 for the synthetic record, which was generated using a multifractal model). For short durations  $d$ , multifractal rainfall models produce nearly constant  $k$  values; hence the decay observed in Figure 4 comes from lack of multifractality for aggregation times  $d$  shorter than about 1 hour. Evidence of such break in scaling can be found for example in Olsson (1995), Onof *et al.* (1996), Menabde *et al.* (1997), de Lima and Grasman (1999), Menabde and Sivapalan (2000) and Koutsoyiannis (2006). The dependence of  $k$  on  $d$  displayed in Figure 4 is especially significant for long return periods, since the tail of the maximum distribution is highly sensitive to  $k$ .

Our conclusion that the separability condition in Eq. 1 does not hold is consistent with findings by other authors on the dependence of the IDF values on duration  $d$ ; see for example Alila (2000) and Brath *et al.* (2003).

One could use annual-maximum methods in which either each duration is treated independently or a non-separable parametric model is specified. However these alternatives are unattractive due to either reduction of the effective sample size from non-pooling of the data for different durations or the difficulty of specifying a non-separable dependence on  $d$  and  $T$ . The marginal and hybrid approaches have the advantage of a larger sample size and the multifractality condition implicitly generates non-separable IDF curves.

#### ***4.2 IDF Curve Estimation and Sensitivity to Outliers***

The first three columns of Figure 5 show the empirical (solid) and estimated (dashed) IDF curves for the three historic rainfall records, when the entire record (i.e. including outlier years) is analyzed by different methods. The empirical return period of the  $i^{\text{th}}$  ranking annual maximum value is calculated using Weibull's (1939) formula  $T_i = (n + 1)/i$ , where  $n$  is the number of years in each record. A similar comparison for the synthetic record is made in the last column of Figure 5, but in this case the empirical IDF curves are replaced with the theoretical ones. The theoretical curves were obtained using the analytical method of Langousis *et al.* (2007), corrected by the continuity factor 1.13.

The return periods of the empirical curves are (2, 8, 25) years for Florence, (2, 8, 52) years for Heathrow Airport, and (2, 8, 50) years for Walnut Gulch. These are also the return periods of the lowest three estimated IDF curves, whereas the return periods of the upper three estimated curves are 100, 1 000, and 10 000 years. The return periods for the synthetic record (for both the theoretical and estimated IDF curves) are 2, 8, 100, 1 000, and 10 000 years. In all cases except Walnut Gulch, the range of  $d$  corresponds to the

scaling range. For Walnut Gulch, longer durations are included to illustrate the local marginal method (LM; dotted lines) in a non-scaling case.

Due to the separability assumption, the IDF curves for different  $T$  estimated by the annual-maximum methods (top two rows) are parallel. For long durations  $d$ , these estimates tend to be more widely spaced than the empirical ones. By contrast, the marginal and hybrid methods produce non-parallel IDF curves that more closely track the empirical ones. Within the scaling range, the LM and MFM methods produce almost identical results; see dashed and dotted lines in the plots in the third row.

Both the Heathrow Airport and Florence records include “outlier years” (1959 and 1970 for Heathrow, 1966 for Florence). Figure 6 shows the sensitivity to outliers by plotting the ratio of the IDF values estimated with and without the outlier years for different estimation methods, durations  $d$ , and return periods  $T$ . The annual-maximum methods CPM and SPM assume separability, as expressed by Eq. 1. In the CPM method, the function  $b(d)$  in Eq. 1 is insensitive to the outlier years, whereas the function  $a(T)$  is highly sensitive. In the SPM method both functions are sensitive to outliers. In either case, the IDF values are affected significantly by the inclusion or exclusion of outlier years. The marginal and hybrid methods (last three rows of Figure 6) are less sensitive, especially for durations  $d$  that during the outlier years did not experience exceptionally intense rainfalls; these are the small  $d$  values for Florence and the large  $d$  values for Heathrow.

### ***4.3 Estimation Bias and Variability for Short Records***

The bias and variability of the estimates when using short rainfall series is examined in Figure 7. For each (method, record) combination, this figure shows the bias and

variability of the 1-hr and 24-hr  $\log_{10}(\text{IDF})$  estimates for  $T = 10, 100, 1\ 000$  and  $10\ 000$  years, when only 5 years of the empirical record or 25 years of the synthetic record are used. No outlier year has been removed. The 5-yr or 25-yr segments used in the analysis are consecutive and non-overlapping, except for the last segment, if the duration of the historical record is not an integer multiple of 5. The records are coded as F = Florence, H = Heathrow Airport, W = Walnut Gulch, and S = synthetic. Different return periods correspond to different bar shadings.

The deviations of the 5-yr  $\log_{10}(\text{IDF})$  estimates from the whole-record estimates [for the synthetic record, the deviations of the 25-yr  $\log_{10}(\text{IDF})$  estimates from the theoretical values] are used to estimate the mean  $b$  (bias), standard deviation  $\sigma$ , and root mean square  $RMS = \sqrt{b^2 + \sigma^2}$  of the  $\log_{10}(\text{IDF})$  estimation error. For example, in the case of Florence, five 5-yr segments are extracted from the 24-yr record (the last one has a 1-yr overlap with the 4<sup>th</sup> segment) and the IDF analysis is repeated for each segment using each method. The estimation errors are obtained by taking the  $\log_{10}$  of the ratio of each 5-yr IDF estimate and the corresponding 24-yr estimate from Figure 5. Therefore, for the actual records, ( $b$ ,  $\sigma$ , and  $RMS$ ) are measures of bias and accuracy relative to the results for the complete but still finite record, whereas for the synthetic data set the same quantities measure the bias and accuracy relative to the true IDF values.

The values of ( $b$ ,  $\sigma$ , and  $RMS$ ) for each IDF estimation method, data set, and return period are shown in Figure 7a for  $d = 1$  hr and in Figure 7b for  $d = 24$  hr. In addition to the SPM and CPM annual-maximum methods and the LM and MFM marginal-distribution methods, two hybrid cases are considered. In one case (MFM/H1) the annual maximum rainfalls are assumed available only for the 5-yr or 25-yr segment of the

record, whereas in the other case (MFM/H2) the annual maximum rainfalls are assumed available for the entire duration of the record (24 years for Florence, 51 years for Heathrow, 49 years for Walnut Gulch, and 1000 years for the synthetic record). The reason for considering the estimator MFM/H2 is that it often happens that the annual maximum record extends back in time further than the continuous record.

As one would expect, method MFM/H2 performs best, but direct comparison of this method with MFM/H1 and the annual-maximum methods would be unfair because results are based on different lengths of the annual-maximum series.

The other methods can be directly compared. The annual-maximum methods perform rather poorly due to high bias, high variance, or both. This is especially true when only 5 years of data are available. In this case the prevalently negative bias is due to the fact that, with a small annual maximum data set, the shape parameter  $k$  of the GEV distribution tends to be underestimated. Hence also the high quantiles of the maximum distribution are underestimated. A small sample size makes the estimation of the GEV parameters ( $k$  in particular) rather erratic and sensitive to outliers; this is why the standard deviation of the error is also large.

On the other hand, the marginal methods and the first hybrid method are nearly unbiased and have moderate variance. When only 5 years of data are available (F, H and W records), the hybrid method performs slightly worse than either LM or MFM, because in this case it is better to correct the marginal estimates by the constant factor 1.13 rather than using the average of the 5 annual maximum values. When 25 years of data are available (S record), the hybrid method performs the best.

## 5. Conclusions

The paper compares several estimators of the IDF curves that are simple enough to be routinely used in practice: currently favored parametric and semi-parametric estimators based on the historical annual maxima, new estimators based on the marginal distribution of rainfall intensity that assume or do not assume multifractal scale invariance, and new hybrid estimators that combine marginal and annual-maximum information.

The annual-maximum estimators are simple but make inappropriate assumptions on the shape of the IDF curves. In addition, their IDF estimates for long return periods are highly variable and sensitive to outlier rainfall events. This is especially true for the semi-parametric method, which imposes loose constraints on the tail of the annual maximum distribution. By contrast, marginal-distribution and hybrid procedures are statistically more stable, more robust against outliers, and applicable also when the rainfall record is short.

A basic assumption that is common to most annual-maximum methods is that the IDF curves are separable in the duration  $d$  and the return period  $T$ . While separability greatly reduces the complexity of the IDF models and their fitting to data, we have found that in reality this condition does not hold. This conclusion is based on ample statistical evidence as well as analysis of multifractal rainfall models for which the exact IDF curves are theoretically known. Marginal-distribution and hybrid methods do not assume separability and are capable of modeling the interactions between  $d$  and  $T$  that are often observed in empirical IDF curves.

Like any other IDF estimation method, marginal distribution procedures present tradeoffs between bias from inappropriate parameterization and variance. For example,



multifractality constrains the way the marginal distribution varies with duration  $d$ . This scaling condition leads to robust IDF estimation procedures but may not accurately apply over a wide range of durations. Hence we have considered a marginal-distribution (LM) method that imposes no scaling condition on the moments. The LM method is very simple. For durations  $d$  in the scaling range, the LM results are only slightly more variable than those under the assumption of multifractality, and the LM method is accurate and robust also outside the scaling range.

The combined use of marginal and annual-maximum information from the rainfall record opens interesting new possibilities. It is intuitively clear that an approach based on marginal distributions is preferable for very short rainfall records, whereas the exclusive use of annual extremes is appropriate in the asymptotic case of infinitely long records. For records of intermediate length, say around 30 years, an effective use of the annual maxima is to correct for the bias of the marginal-distribution results due to the assumption of non-overlapping  $d$  intervals and independence (see bias and variance results in Figure 7, in particular those for the synthetic record). This idea is at the base of our hybrid method.

Again based on Figure 7, our recommendation is that for practical IDF curve estimation one should use the local LM method when the annual maximum series is shorter than about 20 years; otherwise one should use LM/H, the hybrid version of the LM method.

Future work might consider other types of hybrid estimators, in which characteristics of the annual maxima other than the historical average are used to calibrate the marginal-distribution estimates. This may be appropriate when the record of annual maxima is far

longer than the available continuous rainfall record. In some cases historic reports or paleo-information constrain the return period of exceptionally intense rainfall events. For example, for durations  $d$  of about 1-4 days, the extreme event that produced the November 1966 flood in Florence is estimated from historical flood data to have a return period of 500-1000 years. This information can be used to constrain the IDF curves. In addition, comparison could be extended to include peaks over threshold (POT) methods.

Finally we mention the problem of regionalization, i.e. the problem of pooling rainfall data from different sites to refine the IDF estimates at any given geographic location. The marginal-distribution methods proposed in the present study depend on only the first 3 moments of the rainfall intensity  $I(d)$ . Under multifractality, these moments can be further reduced to the moments for a reference duration  $d^*$  and a moment-scaling function  $K(q)$  that characterizes the dependence of the moment of order  $q$  on  $d$ . Hence regionalization requires the spatial mapping of the moments of  $I(d^*)$  and the parameters of  $K(q)$ . Regionalized extensions of the present methods will be considered in future studies.

### **Acknowledgments**

This work was supported in part by the National Science Foundation under Grant No. EAR-0228835, in part by the Alexander S. Onassis Public Benefit Foundation under Scholarship No. F-ZA 054/2005-2006, and in part by the MIUR ex60% fund of Fabio Rossi and Paolo Villani of the University of Salerno. The UK Meteorological Office is acknowledged as provider of the Heathrow Data set which was used as part of collaborative work with Christian Onof. We thank three anonymous reviewers for their useful comments.

## References

- Alila, Y. (2000) Regional Rainfall Depth-duration-frequency Equations for Canada, *Wat. Resour. Res.*, **36**(7): 1767-1778.
- Asquith, W.H. (1998) Depth-Duration Frequency of Precipitation for Texas, Water-Resources Investigations Report 98-4044, U.S. Geological Survey, <http://pubs.usgs.gov/wri/wri98-4044/pdf/98-4044.pdf>.
- Baillon, M., Bessemoulin, P., Goutorbe, J.P., Veysseire, J.M. (2004) Behavior of the Shape Parameter of the Generalized Extreme Value Distribution (GEV) Applied to the Determination of Extreme Precipitation in France, for Accumulation Times from 6min to 10 days, *EMS Annual Meeting Abstract*, **1**(00454).
- Becchi, I. and Castelli, F. (1989) Lettura e archiviazione digitali di registrazioni pluviografiche ad alta risoluzione temporale, Technical Report 1/89, Dep. of Civil Eng., University of Firenze, Italy.
- Bernard, M.M. (1932) Formulas for Rainfall Intensities of Long Durations, *Trans. ASCE*, **96**: 592-624.
- Brath, A., Castellarin, A. and Montanari A. (2003) Assessing the Reliability of Regional Depth-duration-frequency Equations for Gaged and Ungaged sites, *Wat. Resour. Res.*, **39**(12), doi:10.1029/2003WR002399.
- Burlando, P., and Rosso, R. (1996), Scaling and Multiscaling Models of Depth-Duration-Frequency Curves for Storm Precipitation, *J. Hydrol.*, **187**: 45-64.
- Caporali, E., Cavigli, E. and Petrucci, A. (2006) Regional Frequency Analysis of Rainfall extremes in Tuscany (Italy), *International Workshop on Hydrological Extremes*

*Observing and Modelling Exceptional Floods and Rainfalls*, Rende (Cosenza),  
3-4 May 2006

Caporali, E., Rinaldi, M. and Casagli, N. (2005) The Arno River Floods, *Giornale di Geologia Applicata*, **1**: 177-197.

Chow, V.T., Maidment, D.R., and Mays, L.W. (1988) *Applied Hydrology*, McGraw-Hill, New York.

Coles, S.G. (2001) *An Introduction to Statistical Modeling of Extreme Values*, London: Springer.

Coles, S.G. and Tawn, J.A. (1996) A Bayesian Analysis of Extreme Rainfall Data, *Applied Statistics*, **45**: 463-378.

Coles, S.G., Pericchi, L.R. and Sisson, S. (2003) A Fully Probabilistic Approach to Extreme Rainfall Modeling, *Journal of Hydrology*, **273**: 35-50.

Cowpertwait, P.S.P. (1995) A Generalized Spatial-Temporal Model of Rainfall Based on a Clustered Point Process, *Proc. Royal Soc. London, Ser. A*, **450**: 163-175.

Cowpertwait, P.S.P. (1998) A Poisson-Cluster Model of Rainfall: High-Order Moments and Extreme Values, *Proc. Royal Soc. London, Ser. A*, **454**: 885-898.

Davison, A.C. and Smith, R.L. (1990) Models of Exceedance Over High Thresholds, *J. of Royal Stat. Soc., Series B*, **52**(3): 393-442.

de Lima, M. I. P. and Grasman, J. (1999) Multifractal Analysis of 15-min and Daily Rainfall from a Semi-arid Region in Portugal, *J. Hydrol.*, **220**: 1-11.

- Demarée, G. (1985) Intensity-Duration-Frequency Relationship of Point Precipitation at Uccle, Reference Period 1934–1983, *Institut Royal Météorologique de Belgique*, Publication Series A, **116**:1–52.
- Eagleson, P.S. (1970), *Dynamic Hydrology*, McGraw-Hill, New York.
- Fraedrich, K. and Larnder, C. (1993) Scaling Regimes of Composite Rainfall Time Series, *Tellus*, **45A**: 289-298.
- Gumbel, E. J. (1958) *Statistics of Extremes*. Columbia University Press, New York.
- Hershfield, D.M. (1961) Rainfall Frequency Atlas for the U.S. for Durations from 30min to 24hrs and Return Periods from 1 to 100yrs, Technical Paper 40, U.S. Weather Bureau, Washington D.C.
- Hosking, J.R.M. (1992) Moments or L Moments? An Example Comparing two Measures of Distributional Shape, *The American Statistician*, **46**(3): 186-189.
- Katz, R. W., Parlange, M.B. and Naveau, P. (2002) Statistics of Extremes in Hydrology, *Adv. Water Res*, **25**: 1287-1304.
- Koutsoyiannis, D. (2006) An Entropic-Stochastic Representation of Rainfall Intermittency: The Origin of Clustering and Persistence, *Wat. Resour. Res.*, **42**(1), W01401.
- Koutsoyiannis, D., Kozonis, D., and Manetas, A. (1998) A Mathematical Framework for Studying Rainfall Intensity-Duration-Frequency Relationships, *J. Hydrol.*, **206**: 118-135.
- Lang, M., Ouarda, T.B.M.J. and Bobée, B. (1999) Towards Operational Guidelines for Over-Threshold Modeling, *Journal of Hydrology*, **225**: 103-117.

- Langousis A, D. Veneziano, C. Lepore, and P. Furcolo (2007) Multifractal Rainfall Extremes: Theoretical Analysis and Practical Estimation, *Chaos Solitons and Fractals*, doi:10.1016/j.chaos.2007.06.004
- Langousis, A. and Veneziano, D. (2007) Intensity-Duration-Frequency Curves from Scaling Representations of Rainfall, *Wat. Resour. Res.*, **43**, doi: 10.1029/2006WR005245.
- Lovejoy, S., and Schertzer, D. (1990), Our Multifractal Atmosphere: A Unique Laboratory for Nonlinear Dynamics, *Physics in Canada*, July: 62-71.
- Lovejoy, S., and Schertzer, D. (1995) Multifractals and Rain, In: *New Uncertainty Concepts in Hydrology and Hydrological Modelling*, Edited by: Kundzewicz, A.W., Cambridge press, 62-103.
- Madsen, H., Rasmussen, P.F. and Rosbjerg, D. (1997a) Comparison of Annual Maximum Series and Partial Duration Series Methods for Modeling Extreme Hydrologic Events 1. At-site Modeling, *Wat. Resour. Res.*, **33**(4): 747-757.
- Madsen, H., Rasmussen, P.F. and Rosbjerg, D. (1997b) Comparison of Annual Maximum Series and Partial Duration Series Methods for Modeling Extreme Hydrologic Events 2. Regional Modeling, *Wat. Resour. Res.*, **33**(4) : 759-769.
- Menabde, M. and Sivapalan, M. (2000) Modeling of Rainfall Time Series and Extremes Using Bounded Random Cascades and Levy-stable Distributions, *Wat. Resour. Res.*, **36**(11): 3293-3300.

- Menabde, M., Harris, D., Seed, A., Austin, G. and Stow, D. (1997) Multiscaling Properties of Rainfall and Bounded Random Cascades, *Wat. Resour. Res.*, **33**(12): 2823-2830.
- Mohyont, B., Demareé, G.R., Faka, D.N., (2004), Establishment of IDF-curves for Precipitation in the Tropical Area of Central Africa: Comparison of Techniques and Results, *Nat. Haz. Ear. Sys. Sci.*, **4**: 375-387.
- Olsson, J. (1995) Limits and Characteristics of the Multifractal Behavior of a High-Resolution Rainfall Time Series, *Nonlinear processes in Geoph.*, **2**: 23-29.
- Onof, C., Northrop, P., Wheeler, H.S. and Isham, V. (1996) Spatiotemporal Storm Structure and Scaling Property Analysis for Modeling, *J. Geophys. Res.* **101**(D21): 26415-26425.
- Parrett, C. (1997) Regional Analysis of Annual Precipitation Maxima in Montana, Water-Resources Investigations Report 97-4004, U.S. Geological Survey.
- Rosbjerg, D. and Madsen, H. (1992) On the Choice of Threshold Level in Partial Duration Series, *Nordic Hydrological Conference*, Alta, NHP Rep. 30, edited by Gunnar Østrem, pp. 604-615, Coordination Comm. for Hydrol. in the Nordic Countries, Oslo.
- Rosbjerg, D. and Madsen, H. (1995) Uncertainty Measures of Regional Flood Frequency Estimators, *J. Hydrol.*, **167**: 209-224.
- Rossi, F. and Villani, P. (1994) A Project for regional analysis of floods in Italy, In: *Coping with Floods*. Edited by: Rossi, G., Harmancioglu, N. and Yevjevich, V., NATO ASI Series, Kluwer Academic Publishers, Dordrecht, pp. 193-217.

- Sankarasubramanian, A. and Srinivasan, K. (1999) Investigation and Comparison of Sampling Properties of L-moments and Conventional Moments, *J. Hydrol.*, **218**: 13-34.
- Schertzer, D. and Lovejoy, S. (1987) Physical Modeling and Analysis of Rain and Clouds by Anisotropic Scaling of Multiplicative Processes, *J. Geophys. Res.*, **92**: 9693-9714.
- Schmitt, F., Vannistem, S. and A. Barbosa (1998) Modeling of Rainfall Time Series Using Two-state Renewal Processes and Multifractals, *J. Geophys. Res.*, **103 (D18)**: 23,181-23,193.
- Sherman, C.W. (1931) Frequency and Intensity of Excessive Rainfall at Boston, *Trans. ASCE*, **95**: 951-960.
- Singh, V. P. (1992) *Elementary Hydrology*, Prentice-Hall, New Jersey, U.S.A.
- Trefry, C.M., Watkins, D.W. Jr., Johnson, D. (2005) Regional Rainfall Frequency Analyses for the State of Michigan, *J. Hydrol. Eng.*, **10(6)**: 437-449.
- Vaskova, I. and Francis F. (2000), Rainfall analysis and regionalization computing intensity-duration-frequency curves, *Floodaware final report. Programme Climate and Environment 1994-1998. Area 2.3.1: Hydrological and hydrogeological risks. Contract: ENV4-CT96-0293*, Cemagref Editions.
- Veneziano, D. and Furcolo, P. (2002) Multifractality of Rainfall and Intensity-Duration Frequency Curves, *Wat. Resour. Res.*, **38(12)**: 1306-1317.
- Veneziano, D. and Iacobellis, V. (2002) Multiscaling Pulse Representation of Temporal Rainfall, *Wat. Resour. Res.*, **38(8)**: 13.1-13.13.



- Veneziano, D. and Langousis, A. (2005) The Maximum of Multifractal Cascades: Exact Distribution and Approximations, *Fractals*, **13**(4): 1-14.
- Veneziano, D., Langousis, A., and Furcolo, P. (2006) Multifractality and Rainfall Extremes: A Review, *Wat. Resour. Res.*, **42**, W06D15, doi:10.1029/2005WR004716.
- Vogel, R.M. and Fennessey, N.M. (1993) L-moment Diagrams Should Replace Product Moment Diagrams, *Wat. Resour. Res.*, **29**(6): 1745-1752.
- Weibull, W. (1939) A Statistical Theory of the Strength of Materials, *Ing. Vetenskaps Akad. Handl*, Stockholm, **151-3**: 45-55.
- Weiss, L.L. (1964) Ratio of True to Fixed-interval Maximum Rainfall, *J. Hydraul. Div.*, **90**(HY-1): 77-82.
- Willems, P. (2000) Compound Intensity/Duration/Frequency Relationships of Extreme Precipitation for Two Seasons and Two Storm Types, *J. Hydrol.*, **233**: 189-205.
- Young, B.C. and McEnroe, B.M. (2003) Sampling Adjustment Factors for Rainfall Recorded at Fixed Time Intervals, Technical Notes, *J. Hydrol. Eng.*, **8**(5): 294-296.

**Table 1:** Basic statistics of actual and synthetic rainfall records used in the analysis..

**Basic statistics**

	n° years	mean intensity mm/hr	rainy fraction %	mean positive intensity mm/hr
Florence	24	0.0871	7.4	1.18
Heathrow	51	0.0684	8.7	0.78
Walnut Gulch	49	0.0357	2.3	1.53
Synthetic	1000	0.1020	9.6	1.07

**Table 2:** Statistics of 1-hour (a) and 24-hour (b) annual maxima records used in the analysis. The w and w/o columns refer to records with and without outlier years (1966 for Florence, 1959 and 1970 for Heathrow).

**(a) 1-hour annual maxima**

	$\mu$		CV		skewness		L-CV		L-skewness	
	w	w/o	w	w/o	w	w/o	w	w/o	w	w/o
Florence	23.645	23.291	0.376	0.383	1.401	1.653	0.199	0.199	0.206	0.221
Heathrow	14.014	12.902	0.547	0.401	2.439	1.511	0.256	0.209	0.395	0.276
Walnut Gulch	21.930	-	0.428	-	0.803	-	0.236	-	0.135	-
Synthetic	20.810	-	0.483	-	2.880	-	0.228	-	0.312	-

**(b) 24-hour annual maxima**

	$\mu$		CV		skewness		L-CV		L-skewness	
	w	w/o	w	w/o	w	w/o	w	w/o	w	w/o
Florence	2.480	2.270	0.480	0.283	2.808	1.03	0.214	0.155	0.456	0.259
Heathrow	1.670	1.630	0.328	0.319	0.709	0.766	0.185	0.180	0.182	0.187
Walnut Gulch	1.570	-	0.302	-	0.531	-	0.172	-	0.163	-
Synthetic	2.160	-	0.369	-	2.346	-	0.185	-	0.253	-

## Figure Captions

**Figure 1:** Tail plots of the theoretical exceedance probabilities from Eq. 6 with parameters in Eq. 8 and the empirical exceedance probabilities for 1-hr and 24-hr rainfall intensities. The dashed 45-degree lines indicate a perfect match. See text for details.

**Figure 2:** Log-log plots of the normalized empirical moments  $E\{[I(d)/\bar{I}]^q\}$  against  $d$  for  $q = 0, 1, 2, 3, 4$ . Solid lines indicate power-law fits to the moments of order 1, 2 and 3. Dashed lines are the associated moments of order 0 and 4 from Eq. 7.

**Figure 3:** Factors  $R_{cont}$ ,  $R_{dep}$  and  $R$  in Eq. 10 for the Florence, Heathrow, Walnut Gulch and Synthetic records as a function of duration  $d$ . The factors correct the IDF values predicted by the marginal distribution methods for continuity and dependence of rainfall intensity in different  $d$  intervals.

**Figure 4:** Variation of the GEV shape parameter  $k$  with duration  $d$  for the records used in this study and similar results from the literature.

**Figure 5:** Comparison of empirical IDF curves (solid lines) and estimated IDF curves (dashed lines). The estimates are based on the entire records including outlier years. For the synthetic record, the theoretical curves are used instead of the empirical ones. See text for details.

**Figure 6:** Florence and Heathrow Airport records. Ratio of estimated IDF values when outlier years are included and excluded, as a function of duration  $d$  and return period  $T$ .

**Figure 7:** Mean, standard deviation and RMS of the  $\log_{10}(\text{IDF})$  estimation error when using 5-yr subsets of the actual record or 25-yr subsets of the simulated record.

(a)  $d = 1$  hr and (b)  $d = 24$  hr. Varied in a nested way along the horizontal axis are the estimation method, the rainfall record (F = Florence, H = Heathrow Airport, W = Walnut Gulch, and S = synthetic), and the return period (10, 100, 1000 and 10000 years).

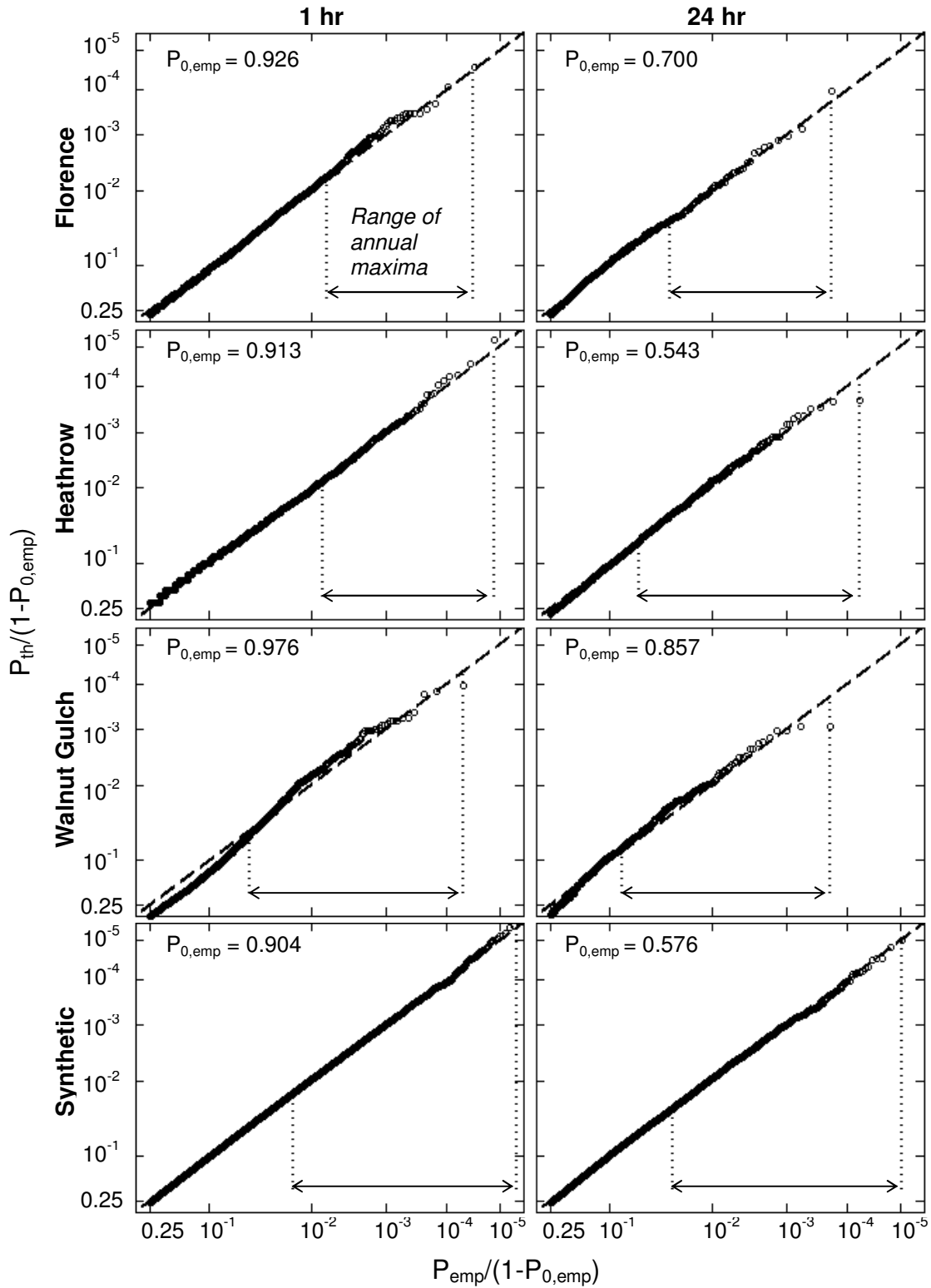


**Figure 1:** Tail plots of the theoretical exceedance probabilities from Eq. 6 with parameters in Eq. 8 and the empirical exceedance probabilities for 1-hr and 24-hr rainfall intensities. The dashed 45-degree lines indicate a perfect match. See text for details.

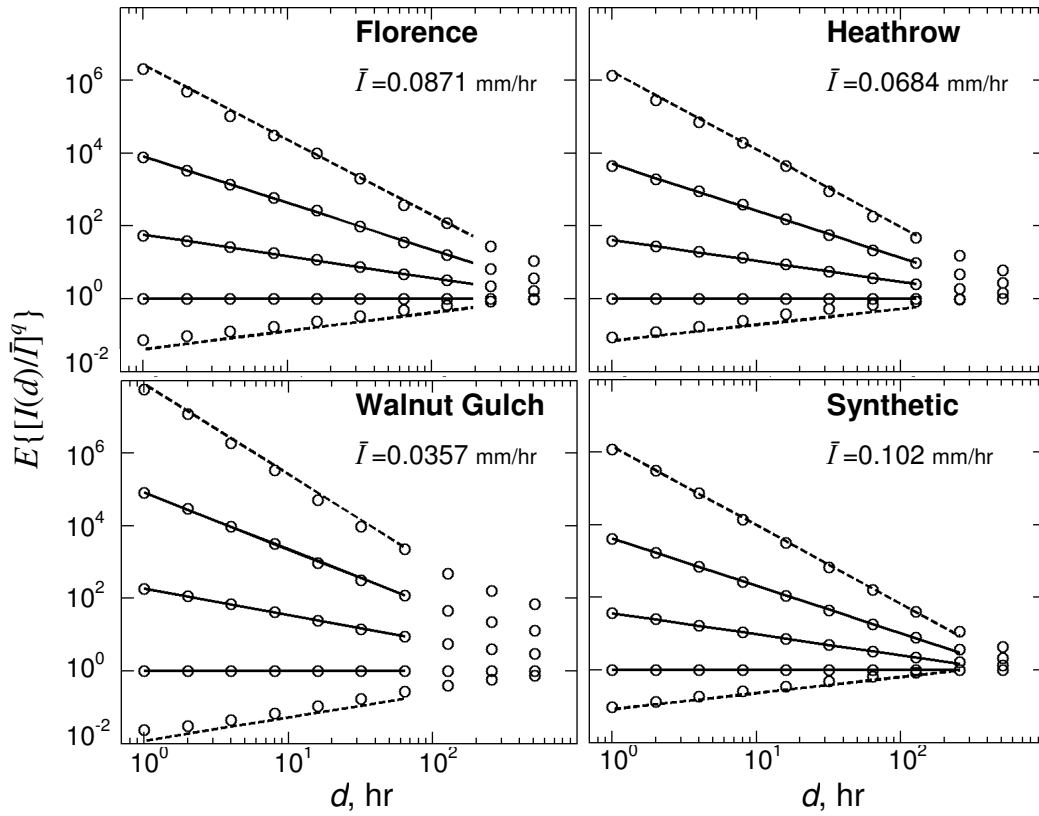


**Figure 2:** Log-log plots of the normalized empirical moments  $E\{[I(d)/\bar{I}]^q\}$  against  $d$  for  $q = 0, 1, 2, 3, 4$ . Solid lines indicate power-law fits to the moments of order 1, 2 and 3. Dashed lines are the associated moments of order 0 and 4 from Eq. 7.

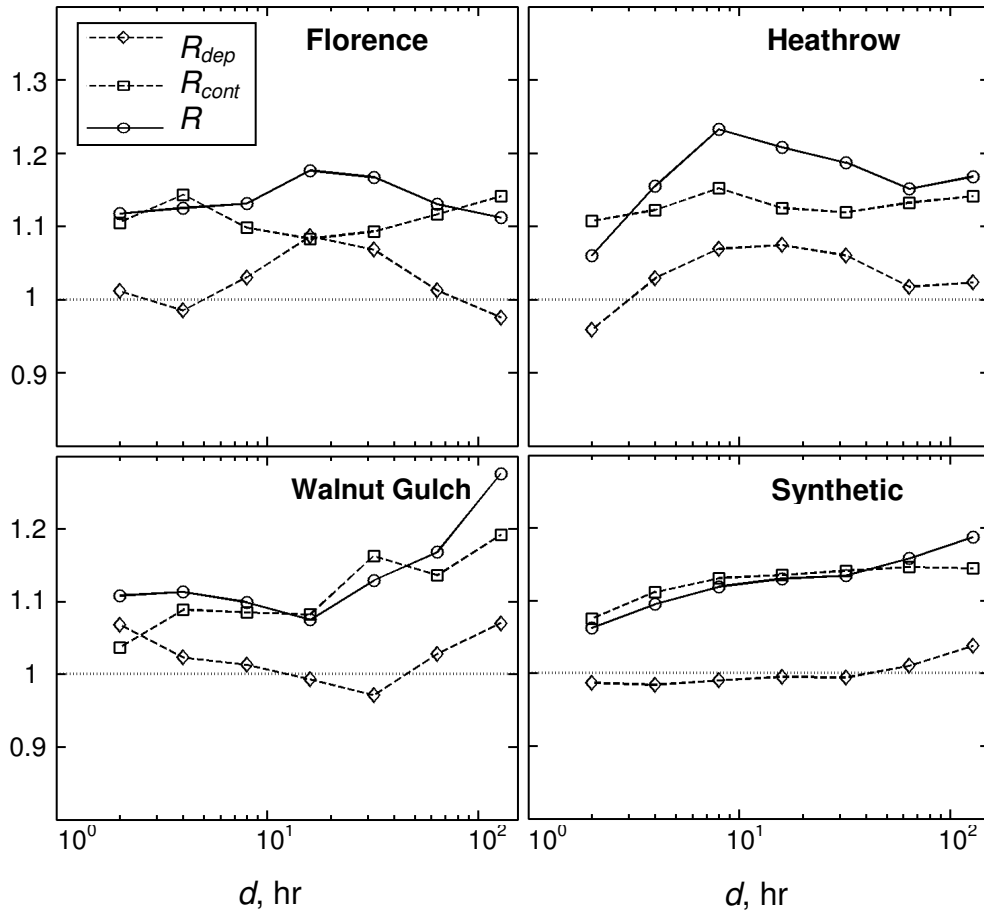


**Figure 3:** Factors  $R_{cont}$ ,  $R_{dep}$  and  $R$  in Eq. 10 for the Florence, Heathrow, Walnut Gulch and Synthetic records as a function of duration  $d$ . The factors correct the IDF values predicted by the marginal distribution methods for continuity and dependence of rainfall intensity in different  $d$  intervals.

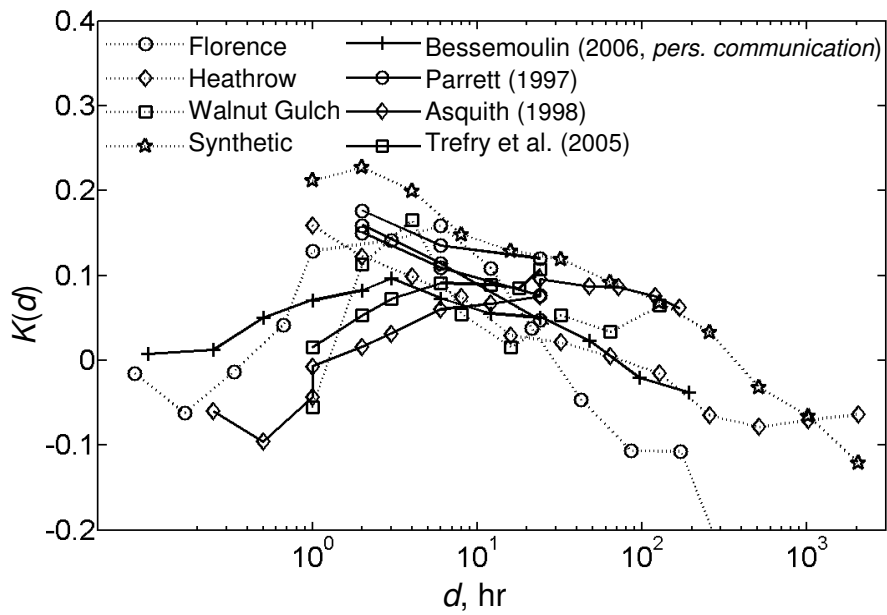


**Figure 4:** Variation of the GEV shape parameter  $k$  with duration  $d$  for the records used in this study and similar results from the literature.



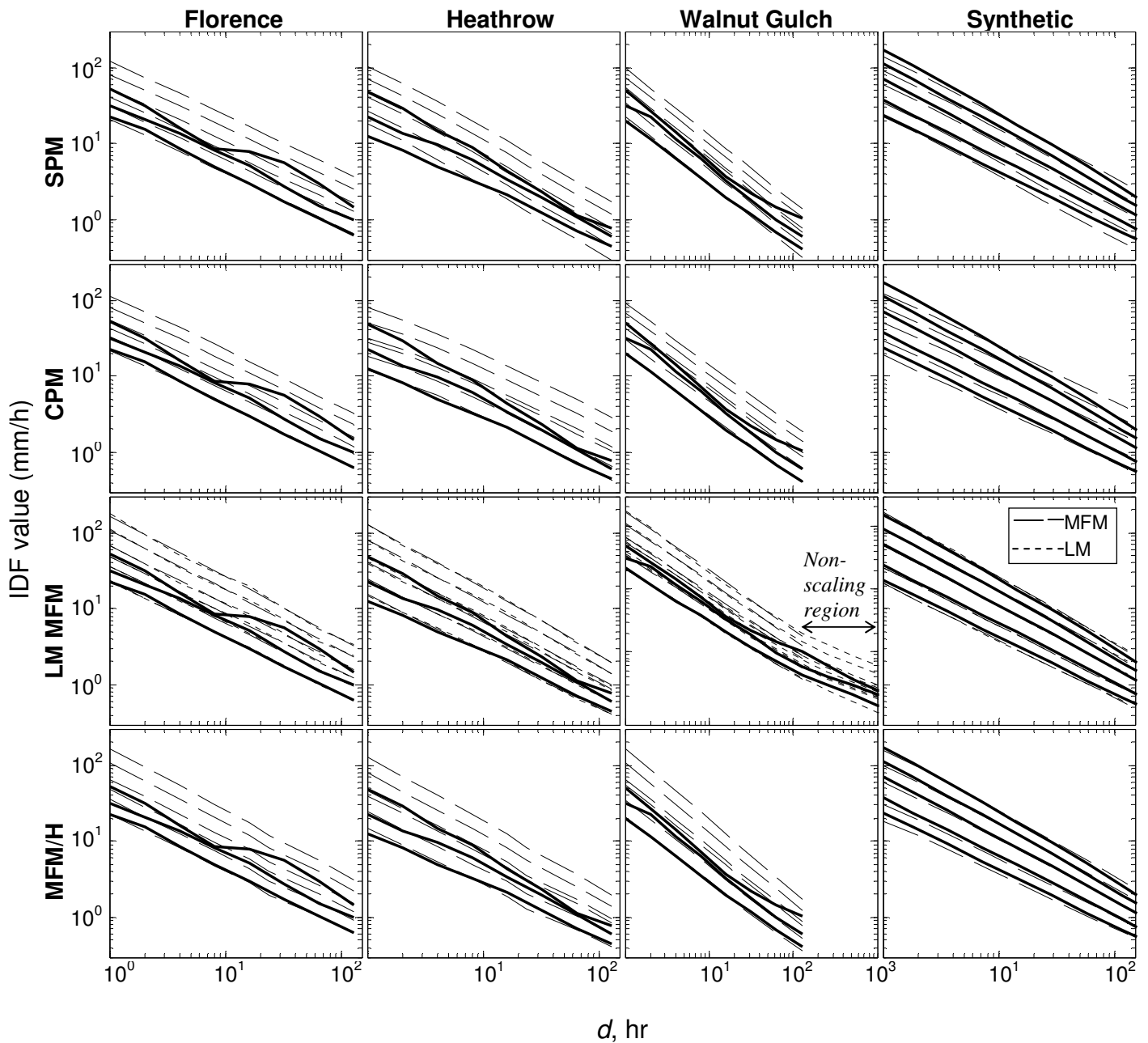


**Figure 5:** Comparison of empirical IDF curves (solid lines) and estimated IDF curves (dashed lines). The estimates are based on the entire records including outlier years. For the synthetic record, the theoretical curves are used instead of the empirical ones. See text for details.

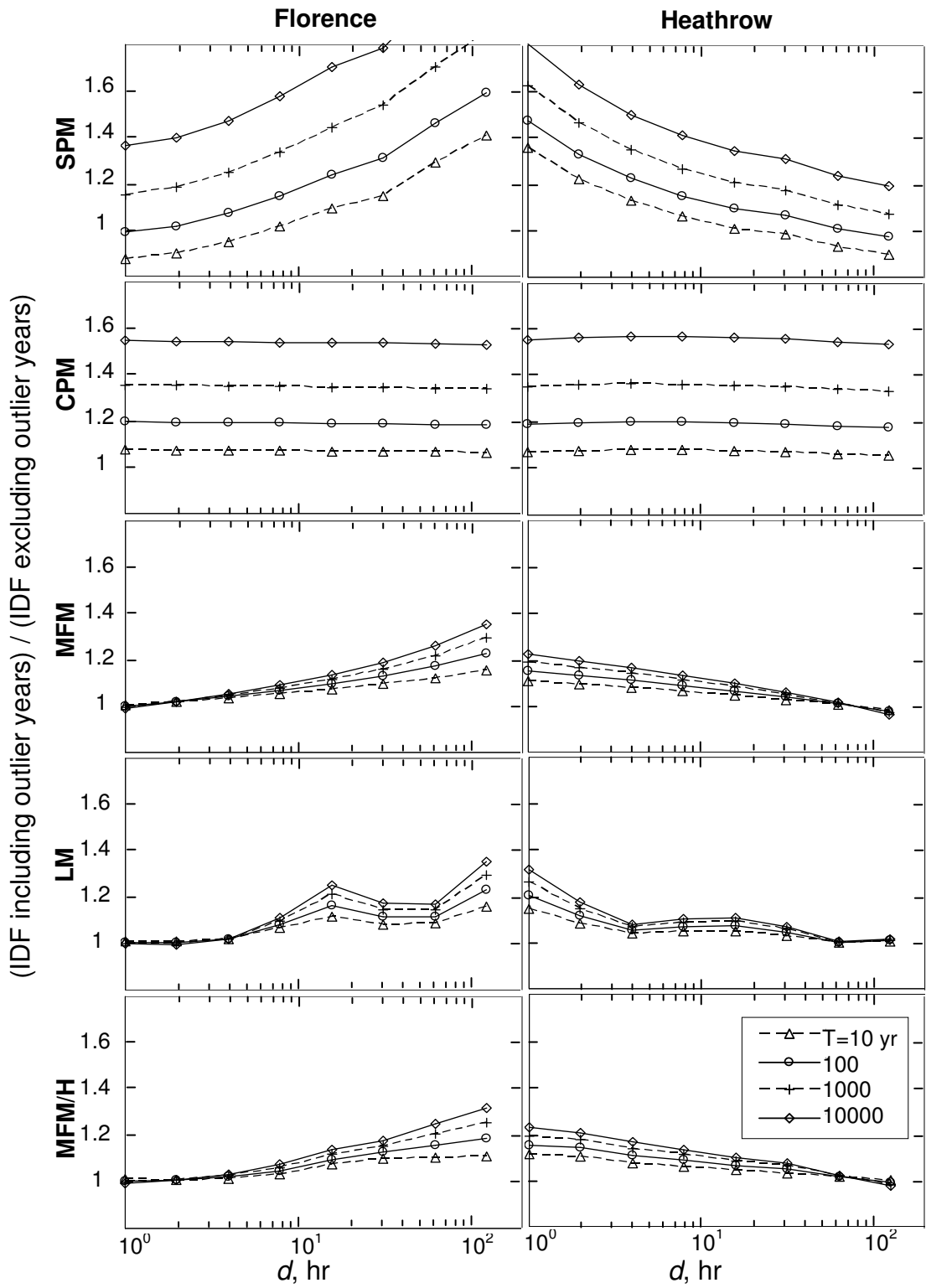


**Figure 6:** Florence and Heathrow Airport records. Ratio of estimated IDF values when outlier years are included and excluded, as a function of duration  $d$  and return period  $T$ .

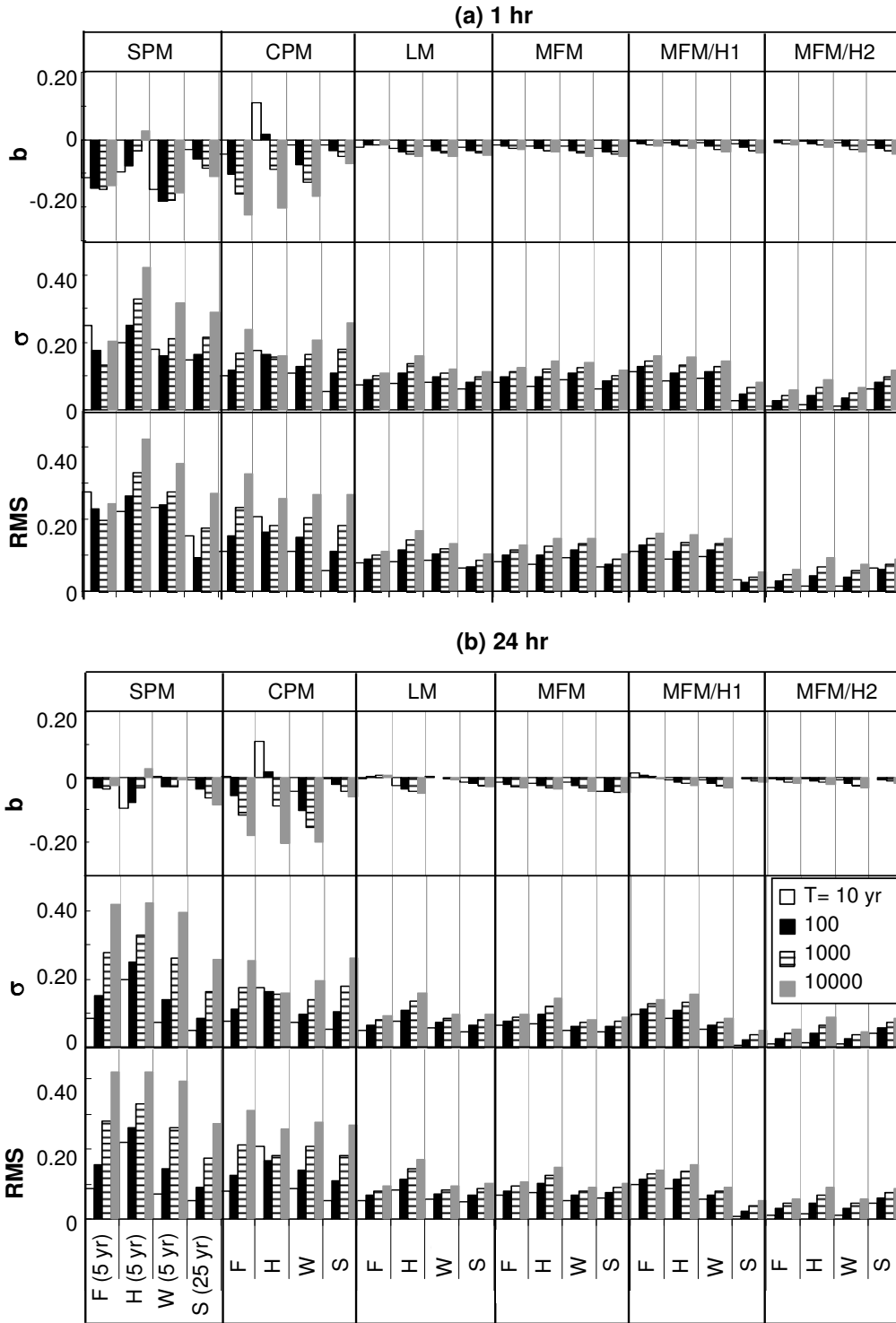


**Figure 7:** Mean, standard deviation and RMS of the  $\log_{10}(\text{IDF})$  estimation error when using 5-yr subsets of the actual record or 25-yr subsets of the simulated record. (a)  $d = 1$  hr and (b)  $d = 24$  hr. Varied in a nested way along the horizontal axis are the estimation method, the rainfall record (F = Florence, H = Heathrow Airport, W = Walnut Gulch, and S = synthetic), and the return period (10, 100, 1000 and 10000 years).